

Apodization along Thickness Direction of Holographic Transmission Grating in Sb-doped $\text{Sn}_2\text{P}_2\text{S}_6$

Y. Wakayama*, A. Okamoto*, A. Tomita*, A. A. Grabar**, K. Sato***, and H. Nihei****

- * Graduate School of Information Science and Technology, Hokkaido University, Kita 14, Nishi 9, Kita-ku, Sapporo, 060-0814 Hokkaido, Japan
- ** Institute of Solid State Physics and Chemistry, Uzhgorod National University, Pidhima 46, 88000 Uzhgorod, Ukraine
- *** Faculty of Engineering, Hokkai-Gakuen University, Minami 26, Nishi 11, Chuo-ku, Sapporo, 064-0926 Hokkaido, Japan
- **** Faculty of pharmaceutical Science, Health Sciences University of Hokkaido, 1757 Kanazawa, Tobetsu-cho, 061-0293 Hokkaido, Japan

Abstract--This report demonstrates a grating apodization method along the thickness direction in a real-time holographic medium for maximizing the diffraction efficiency. Dynamic photo-induced index modulation is examined by the finite-difference beam-propagation method.

I. INTRODUCTION

Transmission-type holographic gratings are applied to many applications, such as the holographic data storage [1], three-dimensional display [2], wavelength filter [3], mode-division multiplexer [4] etc. Increasing the diffraction efficiency (DE) of the gratings is essential to upgrade the performance in most applications. Since the DE increases in proportion to the grating thickness and depth, the development of the holographic media has been focused on how to make a medium with large thickness and large index modulation. However, these methodologies generally bring down the increasing of the optical absorption loss. Therefore, the method of effectively utilizing all over the medium volume is required.

This report investigates the temporal fluctuation of the grating distribution in a real-time holographic medium with purely diffusion nonlinearity [5]. The real-time holograms are dynamically distributed and partially localized. This localization causes a waste area in which deeply modulated gratings are not induced, and spoils the potential of the medium. In this report, we present a grating apodization method along the thickness direction aiming at uniformly activating the whole area of the medium in the case of a Sb-doped $\text{Sn}_2\text{P}_2\text{S}_6$ crystal as an example. In this method, the index distribution can be simply controlled by changing the intensity ratio of the beams for writing the hologram. The apodization effect is clarified by spatial and temporal simulation based on the finite-difference beam-propagation method (FD-BPM) considering dynamically photo-induced index modulation with iterative calculation.

II. SIMULATION MODEL FOR GRATING APODIZATION

The schematic diagram of the simulation for the apodization effect is shown in Fig. 1. The holographic grating is induced in a medium as a real-time hologram by two mutually coherent beams A_{w1} and A_{w2} [Fig. 1(a)]. These beams are assumed as TM-mode beams, and are incident on the left side of the calculation region. The beam propagation with absorption loss is calculated by the wide-angle FD-BPM using Padé (1, 1)

approximant. The index modulation with purely diffusion nonlinearity is calculated using $n^2 = \epsilon_b + \Delta\epsilon$, where n is the refractive index, ϵ_b is the background dielectric constant, and $\Delta\epsilon$ is the change in the dielectric constant related via $\Delta\epsilon = \gamma E$. On the right side of this equation, γ is the real part of the coupling constant, E is the normalized space charge field defined by $E \equiv E_{sc} / E_D$, E_{sc} is the space charge field, E_D is determined by $E_D \equiv k_B T k_D / e = e N_A / e k_D$, and k_D is the Debye wave number. This is solved by the Thomas method using the following equation [6]:

$$E - \frac{1}{k_D^2} \frac{\partial^2 E}{\partial x^2} \left(1 + \frac{1}{k_D} \frac{\partial E}{\partial x} \right)^{-1} = -\frac{1}{k_D} \frac{\partial}{\partial x} \ln I.$$

Here, I is the beam intensity. The FD-BPM is a method for static simulation; however, light passing time through the medium is enough shorter than the response time for carrier inducing. Therefore the temporal evolution is written as

$$E^{t+\Delta t} = E^{t-\Delta t} \exp\left(\frac{-\Delta t}{\tau_{eff}}\right) + E' \exp\left(1 - \frac{-\Delta t}{\tau_{eff}}\right),$$

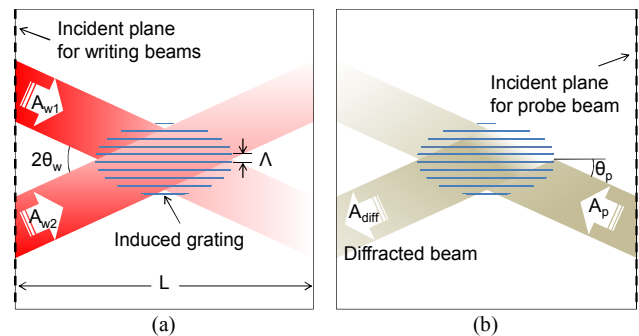


Fig. 1 (a) Writing and (b) probing a holographic grating

TABLE I
Simulation Parameters

Wavelength of writing beams λ_w (μm)	0.633
Wavelength of probe beam λ_p (μm)	0.800
Internal bisect angle between writing beams θ_w ($^\circ$)	3.6
Internal incident angle of probe beam θ_p ($^\circ$)	4.5
Diameters of three incident beams (mm)	0.2
Medium thickness L (mm)	1.0
Refractive index n	3.0
Real part of coupling constant γ (cm^{-1})	20.0
Absorption coefficient at λ_w (cm^{-1})	2.4
Absorption coefficient at λ_p (cm^{-1})	1.0

where the first term of right side is the meaning of erasure term and the second term equals the writing term. Superscripts of $t - \Delta t$, t and $t + \Delta t$ mean the calculation steps for time division, Δt is the time step size, τ_{eff} is an efficient time constant which is determined the ratio of the response time of the medium to the light intensity. A probing procedure is shown in Fig. 1(b). The probe beam propagates from the right to the left side, and diffracts by the induced grating.

In this simulation, the induced index grating is apodized along thickness direction by optimizing the intensity ratio of the writing beams, $q = |A_{w1}|^2 / |A_{w2}|^2$. The intensity ratio q is optimized to maximize the DE of the probe beam. The internal incident angle θ_p is set to $\arcsin(\lambda_p / 2\Lambda)$, where λ_p is the wavelength of probe beam, Λ is grating spacing defined by $\lambda_w / 2\sin(\theta_w)$, θ_w is internal bisect angle between writing beams. The parameters are listed in Table I. The medium parameters are assumed as Sb-doped $\text{Sn}_2\text{P}_2\text{S}_6$ [5]. Here, the wavelengths are different for nondestructive probing.

III. APODIZATION EFFECT

Fig. 2 shows the grating distributions at $q = 0.5$ and 4.0 . The grating modulation around the right side is larger than that around the left side at $q = 4.0$ [Fig. 2 (a)]. On the other hand, the grating distribution is balanced at the four corners of the medium at $q = 0.5$. The grating amplitude for the thickness direction (z -coordinate) at $q = 0.1, 0.5$, and 4.0 are shown in Fig. 3. As a result, the grating distributions were deformed and moved along z -coordinate by changing q . This means that the grating distribution can be apodized by optimizing q . Fig. 4 shows the diffraction efficiencies for various intensity ratios, and determines the optimum intensity ratio as $q = 0.5$. In fact, the grating at $q = 0.5$ was efficiently modulated and distributed in comparison with the grating distributions shown in Figs. 2 and 3. This result indicates that the DE is raised up to 8.2% even in a thin medium of about 1.0 mm thickness.

IV. CONCLUSIONS

This report presents the apodization method along the thickness direction to improve the diffraction efficiency of the transmission-type holographic grating in a photorefractive crystal such as Sb-doped $\text{Sn}_2\text{P}_2\text{S}_6$. This method contributes to reduce the waste area and to activate the entire interactive region by controlling the grating distribution. The effects on the photorefractive crystal of various types will be verified in the future.

ACKNOWLEDGEMENT

This work was supported by a Grant-in-Aid for Scientific Research (21360156) and Global COE Program "Center for Next-Generation Information Technology based on Knowledge Discovery and Knowledge Federation," MEXT, Japan.

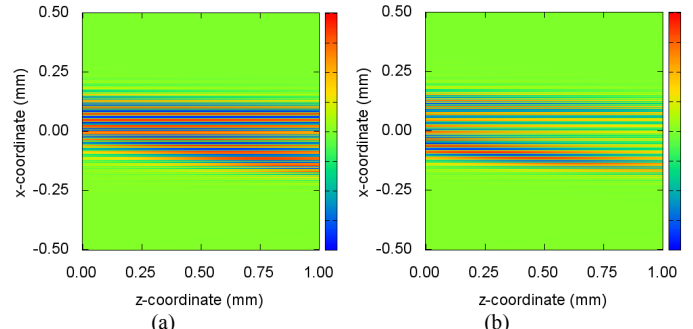


Fig. 2 Grating distribution at $q =$ (a) 0.5 and (b) 4.0

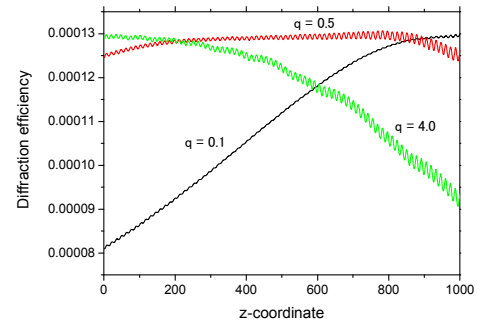


Fig. 3 Amplitude of index modulation for z -coordinate

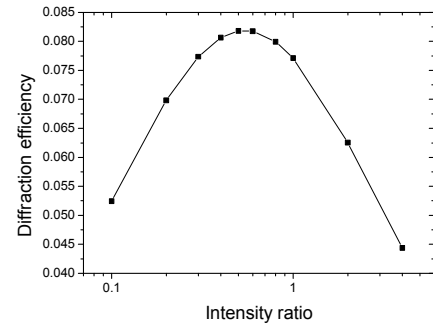


Fig. 4 Diffraction efficiency for intensity ratio

REFERENCES

- [1] J. T. Sheridan, F. T. O'Neill, and J. V. Kelly, "Holographic data storage: optimized scheduling using the nonlocal polymerization-driven diffusion model," *J. Opt. Soc. Am. B*, vol. 21, pp. 1443-1451, 2004.
- [2] P.-A. Blanche, A. Bablumian, R. Voorakaranam, C. Christenson, W. Lin, T. Gu, D. Flores, P. Wang, W.-Y. Hsieh, M. Kathaperumal, B. Rachwal, O. Sddiqui, J. Thomas, R. A. Norwood, M. Yamamoto, and N. Peyghambarian, "Holographic three-dimensional telepresence using large-area photorefractive polymer," *Nature*, vol. 468, pp. 80-83, November 2010.
- [3] Y. Wakayama, A. Okamoto, A. Tomita, and K. Sato, "Ultra-wide tuning range of reconfigurable optical add-drop multiplexer using photorefractive polymer," *Proc. SPIE*, vol. 7958, 79580H(1-8), January 2011.
- [4] A. Okamoto, K. Morita, Y. Wakayama, J. Tanaka, and K. Sato, "Mode division multiplex communication technique based on dynamic volume hologram and phase conjugation," *Proc. SPIE*, vol. 7716-78, pp. 771627(1-10), 2010.
- [5] I. V. Kedyk, P. Mathey, G. Gadret, A. A. Grabar, K. V. Fedyo, I. M. Stoika, I. P. Prits, Y. M. Vysochanskii, "Investigation of the dielectric, optical and photorefractive properties of Sb-doped $\text{Sn}_2\text{P}_2\text{S}_6$ crystals," *Appl. Phys. B*, vol. 92, pp. 549-554, August 2008.
- [6] A. A. Zozulya, M. Saffman, and D. Z. Anderson, "Propagation of Light Beams in Photorefractive Media: Fanning, Self-Bending, and Formation of Self-Pumped Four-Wave-Mixing Phase Conjugate Geometries," *Phys. Rev. Lett.*, vol. 73, no. 6, pp. 818-821, August 1994.